

Tsunami risk estimation for the coasts of Peru and northern Chile

Alexander B. Rabinovich¹, Evgueni A. Kulikov¹, and Richard E. Thomson²

¹*Tsunami Center, Shirshov Institute of Oceanology, Moscow, Russia*

²*Institute of Ocean Sciences, Sidney, British Columbia, Canada*

Abstract. Data for all known tsunamigenic earthquakes and observed tsunami run-up are used to estimate tsunami risk for the coasts of Peru and northern Chile for zones bounded by 0° to 35°S latitude. Tsunamigenic earthquake estimates yield magnitudes of 8.1, 8.4, and 8.7 with corresponding recurrence periods of 50, 100, and 200 years, respectively. According to the “seismic gap” theory, there is a high likelihood of a strong earthquake in the region between 15°S and 24°S. Based on the tsunami run-up data, we expect tsunami wave heights of 13 m for a 50-year return period and 25 m for a 100-year return period. Sophisticated numerical modeling of possible tsunami events is important for estimation of local resonant effects and detailed tsunami-zoning of this region.

1. Introduction

Tsunamis are among the world’s most destructive natural hazards. To mitigate the loss of life and property, the possible impact of tsunami waves must be taken into account prior to major development or construction in seismically active regions of the ocean coast. The past 10 years (1992–2001) have been characterized by anomalously high tsunami activity in the World Ocean. The 17 major tsunamis recorded during this period—including the 21 February 1996 tsunami off Chimbote, northern Peru and the 17 July 1998 tsunami in Papua New Guinea—have been responsible for more than 4000 deaths and extensive property damage. The 1996 Chimbote tsunami was associated with the first large ($M_w > 7$) subduction-zone earthquake between 8 and 10°S in Peru since the 17th century. The devastating Papua New Guinea tsunami killed about 2200 villagers, including more than 230 children (González, 1999). Surprisingly, the large waves associated with the Papua New Guinea tsunami were generated by a relatively small earthquake ($M = 7.1$), indicating that destructive tsunami waves are not confined to earthquakes with extreme magnitudes.

Long-term tsunami prediction (tsunami-zoning) is of key importance to tsunami research, especially for areas of new coastal construction. Construction of complex and/or expensive structures in coastal areas requires reliable estimation of extreme tsunami run-up and run-down. Overestimation of the tsunami risk significantly increases the cost of construction, whereas underestimation of possible tsunami heights may have catastrophic consequences, including widespread destruction of property and loss of life. Tsunami-zoning involves the estimation of maximum tsunami heights, the corresponding inundation (or draw down), and the recurrence times for major tsunami events (cf. Mofjeld *et al.*, 1999).

¹Tsunami Center, Shirshov Institute of Oceanology, Russian Academy of Sciences, 36 Nakhimovsky Prosp., Moscow 117851, Russia (abr@iki.rssi.ru; kulikov@korolev.net.ru)

²Institute of Ocean Sciences, 9860 West Saanich Rd., Sidney, BC V8L 4B2, Canada (ThomsonR@pac.dfo-mpo.gc.ca)

The purpose of this study is to provide preliminary estimates of tsunami crest heights for the coastal area of Peru and northern Chile located between 0° and 35°S . This coast has an extensive history of tsunamigenic earthquakes dating back to July 1586 and remains one of the most seismically active regions in the world. Several major earthquakes and associated tsunamis have occurred in this area over the past few centuries, resulting in severe damage and loss of life. A difficulty with studying tsunamis in this area is a lack of tsunami data, especially for the border region between Peru and Chile. This lack of information is exacerbated by the fact that resonant features of the local topography may significantly affect tsunami waves approaching the coast, resulting in strong spatial variations of tsunami wave heights. Detailed numerical modeling of tsunami waves, combined with observational data (where such data are available) is a common approach for local tsunami zoning (cf. Khrumushin and Shevchenko, 1994; Mofjeld *et al.*, 1999). Because the present study is limited by the fragmentary nature of the historical data, we present only *preliminary* estimates of possible tsunami wave heights. More precise estimates for this area can only be obtained through detailed numerical modeling of regional tsunami waves that takes into account possible resonant features of the regional seafloor topography and coastline.

2. Historical Tsunami Data

The first recorded observations of earthquakes and tsunamis for the Pacific coast of South America date back to the 16th century when Spain established its rule over the New World. Additional descriptions of ancient catastrophic events (earthquakes and sea floods) may be found in Peruvian legends (Soloviev and Go, 1975). Berninghausen (1962) lists 49 tsunamis from 1562 to 1960, from which 23 tsunamis probably impacted the area of study. Further examination of South American tsunamis has been undertaken by Lomnitz (1970), Soloviev and Go (1975), and Lockridge (1985). According to the map of tsunamigenic earthquakes for the period 1562–1960 constructed by Soloviev and Go (1975), almost the entire coast of South America is a zone of high tsunami risk. Based on historical tsunami data, we identify four types of tsunamis capable of impacting the study region: (1) trans-Pacific tsunamis; (2) regional tsunamis; (3) local tsunamis; and (4) landslide-generated tsunamis.

Trans-Pacific tsunamis are tsunamis generated by major earthquakes whose epicenters are located in the so-called “fire-belt of the Pacific,” encompassing areas of Alaska, the Aleutian Islands, the Kamchatka Peninsula, the Kuril Islands, Japan, the Philippines, and Indonesia. Trans-Pacific tsunamis were reported this century for the coast of Peru and Chile in 1946, 1952, 1957, 1960, 1968, 1975, and 1994. Maximum observed wave heights were 3–4 m (Lockridge, 1985).

Regional tsunamis are tsunamis generated by major earthquakes near the coast of South America but relatively far removed from the study region. This includes the main tsunami generation zone off southern Chile. The

1960 Chilean tsunami is an example of this type of tsunami. Waves from this event caused catastrophic damage on the coasts of Hawaii and Japan, and produced 4 m run-up as far away as the northwestern coast of the Sea of Okhotsk (Russia). Regional tsunamis are a serious threat to the coasts of Peru and Chile.

Local tsunamis are those tsunamis generated by major earthquakes in close proximity to the Peru/Chile border. There have been several catastrophic earthquakes in this region—notably the major events of 1604, 1705, 1868, and 1877—which generated tsunami waves with reported wave heights of up to 24–26 m. Clearly, *local tsunamis* are the primary threat to cause damage within the study region.

The possibility of catastrophic *landslide-generated tsunamis* has received little attention for the coast of South America. There have been several cases where relatively small earthquakes have been accompanied by significant tsunamis. For example the 1960 Peruvian earthquake with magnitude $M = 6.9$ produced a tsunami run-up of 9 m (Abe, 1979; Pelayo and Wiens, 1992). One of the possible reasons for these unusually strong tsunamis (compared to the magnitudes of the earthquakes) is that these earthquakes triggered massive submarine landslides on the continental slope of Peru and Chile. Catastrophic tsunamigenic landslides may also occur in the absence of earthquakes, as in the case of the 1994 Skagway, Alaska tsunami (Kulikov *et al.*, 1996). Von Huene *et al.* (1989) found curved scarps cutting the middle slope of the continental margin of northern Peru marking a slip-surface block measuring 20 km by 33 km, which was displaced downslope. If the slip occurred suddenly, a local 50 m-high tsunami would have been generated.

3. Subduction Zones of South America and General Seismicity

Western South America is the only major subduction zone where an entire oceanic slab descends under a continent. Here, the oceanic Nazca Plate subducts beneath the South American continent. Several studies have been devoted to determining the exact subduction geometry of this zone (cf. Kelleher, 1972; Beck and Ruff, 1989; Norabuena *et al.*, 1994). The contact zone between oceanic and continental plates is typically a zone of high seismic activity. With the exception of Japan, the Pacific continental border of South America is the region of highest seismic activity in the world (Lomnitz, 1970). The distribution of earthquake hypocenters clearly indicates that the Nazca Plate is subducting at an inclination of 45–60°, so at 100 km from the trench the depth of earthquake hypocenters are 100 to 200 km. Such deep-focused earthquakes are unlikely to produce tsunami waves, explaining why the epicenters of most of the known tsunamigenic earthquakes are located close to the coastline (Fig. 1).

Kelleher (1972) examined rupture zones of large South American earthquakes and attempted to forecast likely locations of future earthquakes using a seismic gap theory. By mapping the rupture zones of large earthquakes ($M \geq 7.7$), he identified segments of the shallow seismic zones that have not

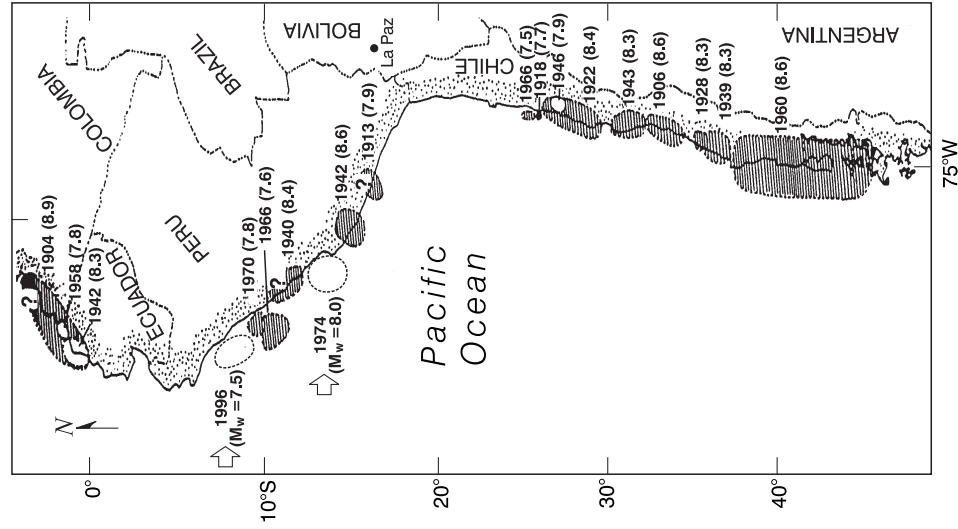


Figure 2: Hatched areas show rupture zones of large ($M \geq 7.5$) South American 20th century earthquakes (from Kelleher (1972)). The 1974 and 1996 earthquakes occurred in the seismic gaps between the 1940 and 1942 rupture zones, and northward from the 1974 rupture zone.

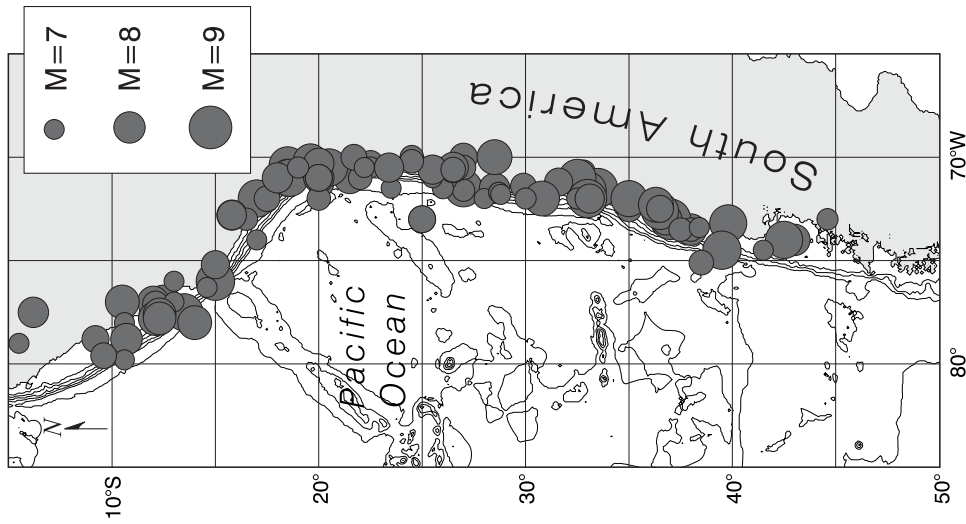


Figure 1: Epicenters of tsunamigenic earthquake sources for the period 1562–1999 for the coasts of Chile and Peru.

Table 1: Computed earthquake magnitudes for different return periods, T_e .

Parameters	Return period, T_e (years)					
	5	10	20	50	100	200
	Earthquake magnitude, M					
M(1552–1999)	6.21	6.63	7.05	7.60	8.01	8.43
M(1900–1999)	7.06	7.38	7.69	8.11	8.42	8.73

ruptured in many decades (Fig. 2). Following “seismic gap theory,” these gaps between rupture zones tend to be the focus of large-magnitude earthquakes. One of the zones detected by Kelleher (1972) as an area of strong future earthquakes is a segment along the Peru Trench located between the rupture zones of the 1940 and 1942 earthquakes (12–14°S) (see Fig. 2). Two years after publication of Kelleher’s 1972 paper, a large tsunamigenic earthquake with $M_w = 8.0$ occurred in this exact area (Fig. 2); Kelleher’s forecast was very precise (cf. Dewey and Spence, 1979; Beck and Ruff, 1989).

In light of Kelleher’s prediction, the huge seismic gap between 15° and 24°S has significant importance. In the past, several strong tsunamigenic earthquakes occurred in this area, including the 1604 First Arica Earthquake with a magnitude 8.5 at 17°S, a large earthquake in 1705 at 18.6°S, the Second (Great) Arica Earthquake of 1868 with a magnitude 8.5, and the 1877 Tarapaca Earthquake at 19.6°S with a magnitude of 8.3. As emphasized by Lockridge (1985), a large-magnitude event has not occurred in this area since 1877, making this region a seismic gap with the potential to produce future large earthquakes ($M = 8.0$ – 8.5) and damaging tsunamis. Tsunami heights associated with the earthquakes of 1604, 1705, 1868, and 1877 were 16, 8, 16, and 24 m, respectively. Thus, even by crude estimates, tsunamis with *wave heights of about 16 m will occur in this region once every 100 years*. In accordance with the seismic gap theory, a strong event is likely to occur in the near future.

Based on the earthquake data for the period 1552–1999 (Fig. 1), earthquake recurrence times (T_e in years) and magnitudes (M) are related by the empirical relation:

$$M = 1.38 \log(T_e) + 5.25 \quad (1)$$

The corresponding regression relation between M and T_e for the post-1900 earthquake data is:

$$M = 1.05 \log(T_e) + 6.33. \quad (2)$$

As a result of improved earthquake statistics for the 20th century, there is a significant increase in all estimated values compared with the pre-1900 data, despite the fact that during the last 100 years there have been no strong earthquakes in the study region similar to those observed in the 17th or 19th centuries (the epicenter of the 1960 Chile Earthquake was located on latitude 41°S, outside our study region). Computed values of M are presented in Table 1.

4. Estimates of Tsunami Run-Up Heights from Tsunami Data

We used data from the World Data Center-A (Boulder, Colorado) to estimate tsunami statistics and heights for the coasts of Peru and northern Chile. Two types of database search were conducted: “Tsunami Event” and “Tsunami Run-up.” We used both types of modes and selected all data for the Pacific coast from 0°S to 35°S, including Peru, northern Chile, and Ecuador.

From the “Tsunami Event” search, we selected 180 events for the period 1562 to 1996. From the “Tsunami Run-up” search mode, we found more than 400 run-up values for different coastal points. Instrumental recording of sea level variations began systematically only in the 20th century, so that the quality of the recent and historical data is markedly different. Basically, we have statistics for “small” tsunami events (wave heights less than 1–2 m) for the last 80–90 years.

Figure 3 shows the spatial distribution of historical tsunami run-up along the coasts of Peru and northern Chile. Despite the irregular distribution of reporting sites along the coast, the tsunami risk for the whole coast seems to be *quasi-constant* in that it does not appear to depend on latitude. This can be explained by the almost uniform spatial distribution of tsunami sources (earthquake epicenters) (Fig. 1) and the relatively uniform structure of seafloor topography along the coast. Only in the northern part of the region (the Ecuador coast) is there a diminishing risk of tsunamis, presumably related to the coastal shielding of tsunami waves originating in the south. Run-up heights cannot be expected to be uniformly distributed along the coast for a *single* tsunami source. Maximum run-up heights are normally observed near the source, as evident from Fig. 4 for the 1868, 1877, 1966, and 1996 tsunamis. Statistically, tsunami heights decrease away from the source region according to $R^{-\frac{1}{2}}$, where R is the distance from the source. However, for purposes of this analysis, the statistical distribution of tsunami run-up heights (for all events) is treated as uniform from 5° to 35° latitude.

The spatial distribution of tsunami heights along the coast may be significantly modified by local topography, coastal irregularities, shelf resonance effects, and other topographical factors (see, for example, Fig. 3 in Bourgeois *et al.*, 1999). Thus, to correctly estimate tsunami heights for a selected point, the above effects need to be examined for a large segment of the neighboring coasts. A combination of careful examination of the coastal observational data and numerical modeling of tsunami propagation and transformation would significantly improve the quality and reliability of any data-based analysis (cf. Khrumushin and Shevchenko, 1994; Mofjeld *et al.*, 1999).

Figure 5 is a stick plot of tsunami run-up recorded in the Peru region from 1562 to 1996. The time series appears to be strongly stochastic with stationary variability. For this reason, we use statistical analysis of extremes originally developed for river flood events. Figure 6 presents graphs of tsunami height distribution (recurrence times) based on: (1) A statistical analysis of all data from 1562 to 1996; and (2) a statistical analysis of recent data from 1906 to 1996. According to this figure, the historical data from

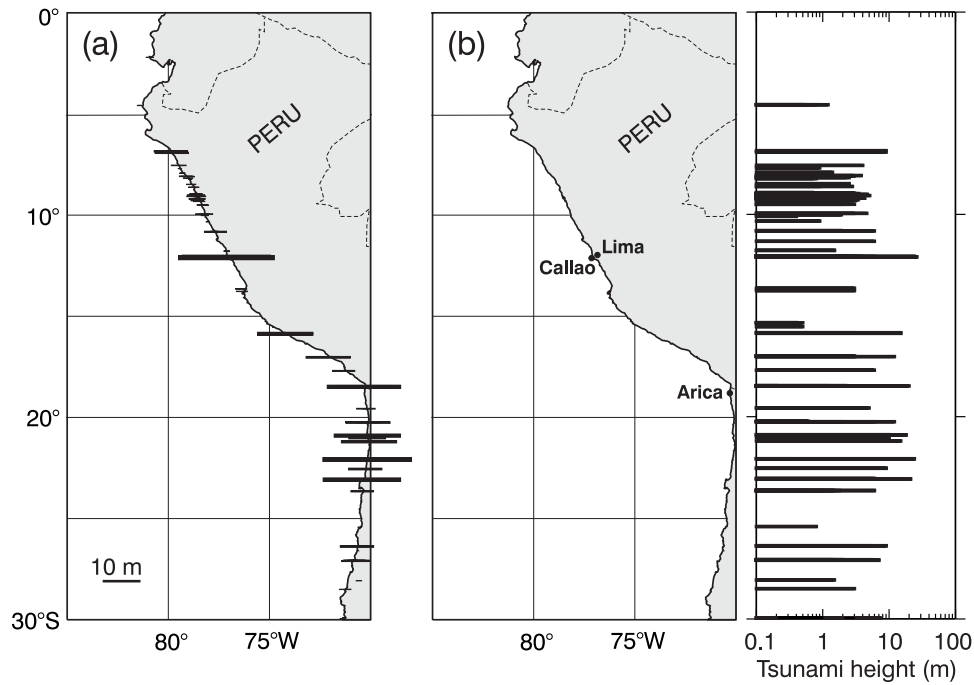


Figure 3: Distribution of tsunami run-up heights along the coasts of Peru and northern Chile from 1562 to 1996.

1562 to 1900 are devoid of small tsunamis with run-up heights less than 1 m. In the 20th century, coinciding with the beginning of sea level surveys and instrumental recording, the numbers of relatively frequent small tsunamis increases dramatically, similar to the numbers of earthquakes. For this reason the distribution for the full data set falls below the distribution for recent data for small heights (less than 2–3 m). However, for large run-up (larger than 3–4 m) both graphs merge. There is a straight line asymptotic approximation for large tsunami run-ups given by the function $h \sim T^p$, where h is the tsunami run-up and T is the return period, typical of lognormal distributions of the form (Gumbel, 1962):

$$f(x) = \frac{1}{x\sqrt{2\pi}} \exp\left(-\frac{\ln^2(x)}{2}\right) \quad (3)$$

Approximation (3) has been used to estimate tsunami run-up heights for the basic return periods of 5, 10, 20, 50, and 100 years (Table 2).

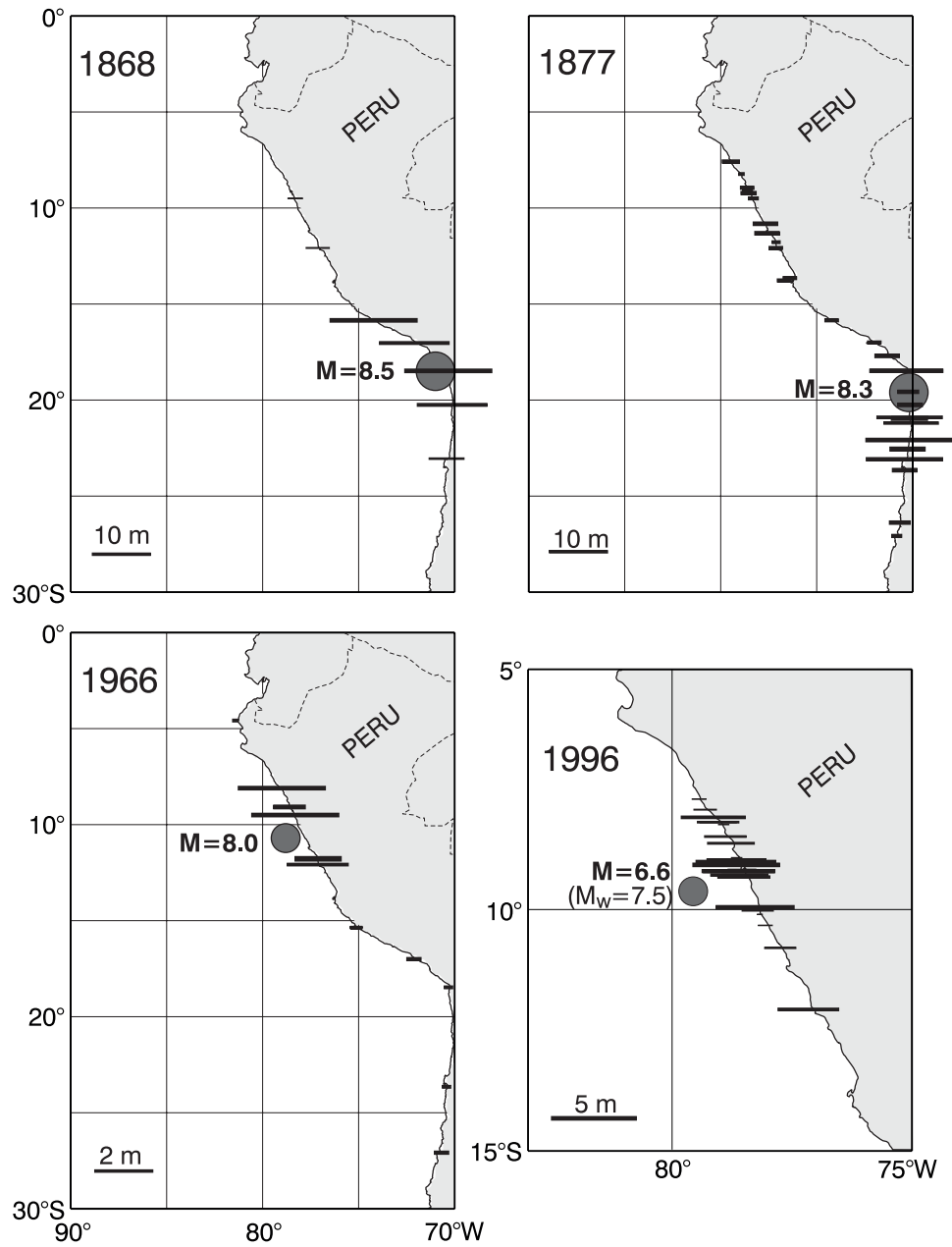


Figure 4: Distribution of tsunami run-up heights along the coasts of Peru and northern Chile for (a) the 1868 Second Arica Earthquake with $M = 8.5$; (b) the 1877 Tarapaca earthquake with $M = 8.3$; (c) the 1966 Peru earthquake with $M = 8.0$; and (d) the 1996 Chimbote earthquake with $M = 6.6$ ($M_w = 7.5$).

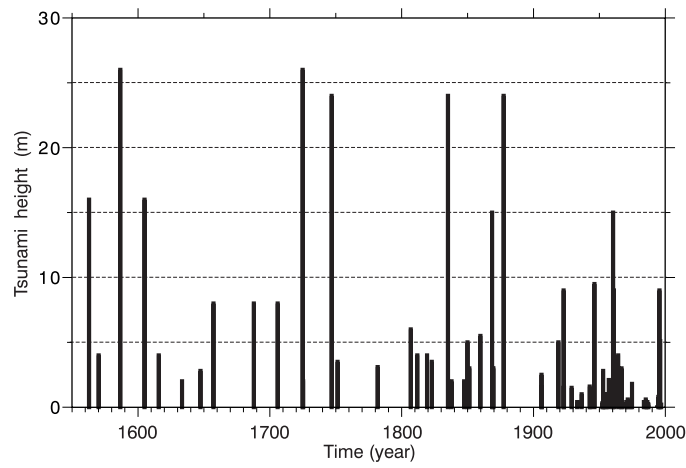


Figure 5: Time distribution of historical tsunami events for the coast of Peru from 1562 to 1996.

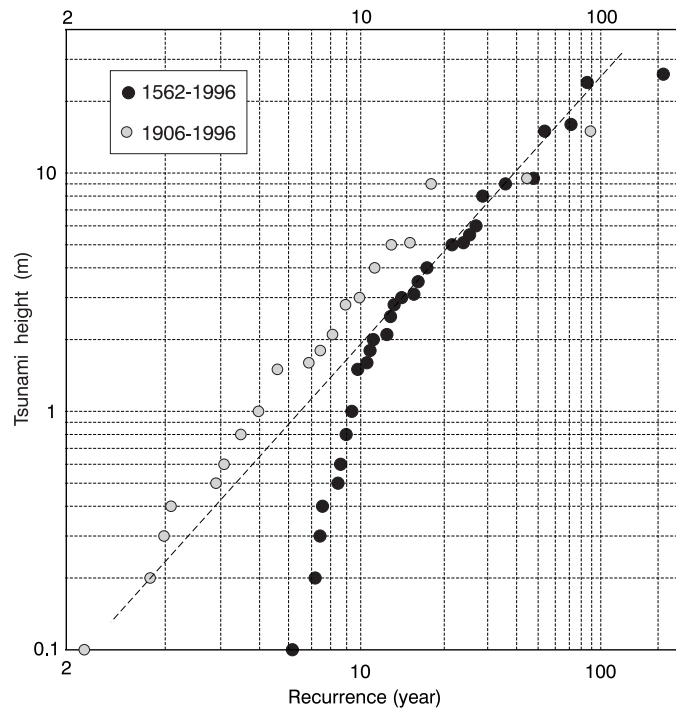


Figure 6: Recurrence time of tsunami run-up heights calculated for historical tsunami records for the periods 1562 to 1996 (all data) and 1906 to 1996 (recent data).

Table 2: Tsunami run-up heights, h , and corresponding recurrence times, T_e .

Parameter	Return period, T_e (years)				
	5	10	20	50	100
Tsunami height (m)	1.30	2.99	5.69	13.30	25.29

5. Conclusions

We conducted a thorough risk analysis based on a detailed examination of all known tsunamigenic earthquakes and observed tsunami run-up for the coasts of Peru and northern Chile for zones bounded by 0° to 35°S latitude. Calculations from the *tsunamigenic earthquake estimates* indicate earthquake magnitudes 8.1, 8.4, and 8.7 corresponding to 50, 100, and 200-year recurrence periods, respectively.

Preliminary findings from the tsunami run-up data indicate that the “Likely Case” event—corresponding to a 50-year recurrence period—is 13 m. Adding a 2 m tide increases this estimate to approximately 15 m. The “Worst Case” tsunami run-up—corresponding to a 100-year return event—is 25 m (27 with a 2 m tide).

The region between 15°S and 24°S , straddling the Peru/Chile border, lies in a “seismic gap” which has not experienced an earthquake since 1877. Thus, it has high potential for a major earthquake of magnitude greater than 8.0. The earthquake of 1877 generated tsunami run-up as much as 25 m for the region of Arica-Ilo.

6. References

- Abe, K. (1979): Size of great earthquakes of 1837–1974 inferred from tsunami data. *J. Geophys. Res.*, 84(B4), 1561–1568.
- Beck, S.L., and L.J. Ruff (1989): Great earthquakes and subduction along the Peru trench. *Phys. Earth Planet. Int.*, 57, 199–224.
- Berninghausen, W.H. (1962): Tsunamis reported from the west coast of South America 1562–1960. *Bull. Seismol. Soc. Am.*, 52(4), 915–921.
- Bourgeois, J., C. Petroff, H. Yeh, V. Titov, C. Synolakis, B. Benson, J. Kuroiwa, J. Lander, and E. Norabuena (1999): Geologic setting, field survey and modeling of the Chimbote, northern Peru, tsunami of 21 February 1996. *Pure Appl. Geophys.*, 154(3/4), 513–540.
- Dewey, J.W., and W. Spence (1979): Seismic gaps and source zones of recent large earthquakes in coastal Peru. *Pure Appl. Geophys.*, 117, 1148–1171.
- Go, Ch.N., V.M. Kaistrenko, and K.V. Simonov (1985): A two-parameter scheme for tsunami hazard zoning. *Mar. Geod.*, 9(4), 469–476.
- González, F.I. (1999): Tsunami! *Scientific American*, 280(5), 56–65.
- Gumbel, E. (1962): *Statistics of Extremes*. Columbia University Press, New York.
- Heinrich, P., J.-M. Gomez, S. Guibourg, and P.F. Ihmle (1998): Modeling of the February 1996 Peruvian tsunami. *Geophys. Res. Lett.*, 25(14), 2687–2690.
- Kelleher, J.A. (1972): Rupture zones of large South American earthquakes and some predictions. *J. Geophys. Res.*, 77(11), 2087–2103.

- Khramushin, V.N., and G.V. Shevchenko (1994): A method of detailed tsunami zoning for coastal Aniva Bay. *Oceanology*, 34(2), 192–197.
- Kulikov, E.A., A.B. Rabinovich, R.E. Thomson, and B.D. Bornhold (1996): The landslide tsunami of November 3, 1994, Skagway Harbor, Alaska. *J. Geophys. Res.*, 101(C3), 6609–6615.
- Lockridge, P.A. (1985): *Tsunamis in Peru-Chile*. World Data Center A for Solid Earth Geophysics, Report SE-39, U.S. Department of Commerce, NOAA, Boulder, Colorado, 97 pp.
- Lomnitz, C. (1970): Major earthquakes and tsunamis in Chile during the period 1535 to 1955. *Geolog. Rundsch.*, 59(3), 938–960.
- Mofjeld, H.O., F.I. González, and J.C. Newman (1999): Tsunami prediction in U.S. coastal regions. In *Coastal and Estuarine Studies*, 56, AGU, 353–375.
- Norabuena, E.O., J.A. Snoke, and D.E. James (1994): Structure of the subducting Nazca Plate beneath Peru. *J. Geophys. Res.*, 99(B5), 9215–9226.
- Pelayo, A.M. and D.A. Wiens (1992): Tsunami earthquakes: slow thrust-faulting events in the accretionary wedge. *J. Geophys. Res.*, 97(B11), 15,321–15,337.
- Planning for Risk: Comprehensive Planning for Tsunami Hazard Areas (1988): Prepared by Urban Regional Research for the National Science Foundation, 246 pp.
- Soloviev, S.L., and Ch.N. Go (1975): *Catalogue of Tsunamis on the Eastern Shore of the Pacific Ocean*. Nauka Publ. House, Moscow, 204 pp. (in Russian; English translation: Canadian Transl. Fish. Aquatic Sci., No. 5078, Ottawa, 293 pp., 1984).
- Von Huene, R., J. Bourgeois, J. Miller, and G. Pautot (1989): A large tsunamogenic landslide and debris flow along the Peru Trench. *J. Geophys. Res.*, 94(B2), 1703–1714.